



Published in final edited form as:

*J Biol Chem.* 2004 December 3; 279(49): 51545–51553.

## Macrophage tropism of HIV-1 depends upon efficient cellular dNTP utilization by reverse transcriptase<sup>+</sup>

Tracy L. Diamond<sup>1</sup>, Mikhail Roshal<sup>1</sup>, Varuni K. Jamburuthugoda<sup>2</sup>, Holly M. Reynolds<sup>1</sup>, Aaron R. Merriam<sup>1</sup>, Kwi Y. Lee<sup>1</sup>, Mini Balakrishnan<sup>2</sup>, Robert A. Bambara<sup>2,3</sup>, Vicente Planelles<sup>4</sup>, Stephen Dewhurst<sup>1,3</sup>, and Baek Kim<sup>1,\*</sup>

<sup>1</sup>Department of Microbiology and Immunology, <sup>2</sup>Department of Biochemistry and Biophysics, and <sup>3</sup>Cancer Center, University of Rochester Medical Center, 601 Elmwood Avenue Box 672, Rochester, New York 14642, <sup>4</sup>Department of Pathology, University of Utah School of Medicine, 30 N. 1900 East, SOM C210, Salt Lake City, UT 84132.

### Abstract

Retroviruses utilize cellular dNTPs to perform proviral DNA synthesis in infected host cells. Unlike oncoretroviruses, which replicate only in dividing cells, lentiviruses, such as HIV-1 and SIV, are capable of efficiently replicating in non-dividing cells (terminally differentiated macrophages) as well as dividing cells (i.e. activated CD4<sup>+</sup> T cells). In general, non-dividing cells likely have low cellular dNTP content, compared to dividing cells. Here, by employing a novel assay for cellular dNTP content, we determined the dNTP concentrations in two HIV-1 target cells, macrophages and activated CD4<sup>+</sup> T cells. We found that human macrophages contained 130–250 fold lower dNTP concentrations than activated human CD4<sup>+</sup> T cells. Biochemical analysis revealed that, unlike oncoretroviral reverse transcriptases (RTs), lentiviral RTs efficiently synthesize DNA even in the presence of the low dNTP concentrations equivalent to those found in macrophages. In keeping with this, HIV-1 vectors containing mutant HIV-1 RTs, which kinetically mimic oncoretroviral RTs, failed to transduce human macrophages, despite retaining normal infectivity for activated CD4<sup>+</sup> T cells and other dividing cells. These results suggest that the ability of HIV-1 to infect macrophages, which is essential to establishing the early pathogenesis of HIV-1 infection, depends, at least in part, upon enzymatic adaptation of HIV-1 RT to efficiently catalyze DNA synthesis in limited cellular dNTP substrate environments.

### Abbreviations

dNTP, 2'-deoxynucleoside 5'-triphosphate; T/P, template-primer complex; RT, reverse transcriptase; HIV-1, human immunodeficiency virus Type 1; SIV, simian immunodeficiency virus; MuLV, murine leukemia virus; AMV, avian myeloblastosis virus

### Introduction

Cellular dNTP levels serve as a biomarker for the replicative capacity of mammalian cells (review(1)). Consistent with this, numerous studies have reported that dNTP contents in cancer cells and transformed cell lines are 3–10 fold elevated compared to normal cells and that dividing cells have higher dNTP contents than non-dividing cells (1–6). Cellular dNTP levels

<sup>+</sup>This work was supported by research grants, AI49781 (to B.K.), P01 MH64570 and S11 NS43499 (to S.D.), GM49573 (to R.A.B.), AI49057 (to V.P) and training grant T32 AI49815 (to M.R. and T.L.D.) from the National Institutes of Health.

\*Corresponding author Baek Kim, Ph.D., Department of Microbiology and Immunology, University of Rochester, 601 Elmwood Avenue Box 672, Rochester, NY 14642, Tel: (585) 275-6916, Fax: (585) 473-9573, Email:baek\_kim@urmc.rochester.edu.

also fluctuate during the cell cycle and upon DNA damage, when replication and repair DNA synthesis levels are altered (6–10). In addition, many viruses utilize cellular dNTPs in order to carry out their replicative cycle. These include lentiviruses, such as the human and simian immunodeficiency viruses (HIV-1 and SIV), which are unique among retroviruses in their ability to infect both non-dividing (e.g., terminally differentiated macrophages (11)) and dividing (e.g., activated CD4<sup>+</sup> T cells) cells. Changes in cell tropism between macrophages and T cells that occur during the course of lentiviral infection are closely related with immunological and clinical manifestations of lentivirus infection (i.e. CD4<sup>+</sup> T cell decrease and AIDS). In contrast to lentiviruses, oncoretroviruses productively replicate only in dividing cells (11,12). Therefore, it is intriguing to consider how lentiviral DNA polymerases may have evolved to efficiently replicate in quiescent cells (i.e., terminally-differentiated/non-dividing macrophages) that presumably contain low levels of dNTPs.

In this study, we established a sensitive dNTP assay to measure dNTP concentrations in primary HIV-1 susceptible host cells. Biochemical analysis revealed that HIV-1 reverse transcriptase (RT) efficiently performs processive DNA synthesis under reaction conditions that contained dNTP concentrations equivalent to those found in macrophages. In contrast, oncoretrovirus RTs were unable to efficiently polymerize under these conditions. Finally, we designed pseudotyped HIV-1 virus vectors that contained either wild-type RT or RTs with mutations that affected dNTP binding affinity. Analysis of reporter gene expression in vector-infected target cells revealed that the mutant constructs could transduce only actively dividing cells (cell lines, primary activated T cells), whereas the wild type vectors could transduce both dividing and non-dividing (macrophage) host cells. Collectively, these data provide evidence that the unique ability of HIV-1 to infect non-dividing cells depends at least in part upon the evolutionary adaptation of its reverse transcriptase to function under conditions of limiting dNTP availability.

## Experimental Procedures

**Materials:** Oligonucleotides were purchased from Integrated DNA Technologies (Iowa). Hexahistidine-tagged p66/p66 RT homodimers derived from HIV-1 (HXB2 (13,14)) and SIV (SIVMNECL8 (15)), or RT monomers of MuLV (16), were isolated from bacterial overexpression systems described in our previous studies. AMV RT and KF were purchased from Stratagene (La Jolla, CA) and New England Biolabs, Inc. (Beverly, MA), respectively.

**Single nucleotide incorporation assay:** Four different 19-mer DNA templates containing sequence variations (**N**) at the 5' end nucleotide (5'-**N**TGGCGCCCGAACAGGGAC-3') were individually annealed to an 18-mer DNA primer (5'-GTCCCTGTTCGGGCGCCA-3'), <sup>32</sup>P-labeled at its 5' end (template:primer, 4:1). The nucleotide at the 5' end of the primer determines the dNTP to be measured. The primer (160 pmole in 80 µl) was labeled using 40 units of T4 polynucleotide kinase (New England BioLabs, Inc., MA) with 80 µCi α-<sup>32</sup>P-ATP (Amersham, NJ) for 30 min at 37°C. An additional 40 units of T4 polynucleotide kinase was added for an additional 30 min period of labeling. After heat inactivation (95°C, 10 min), the labeled primer was split into four separate tubes annealed with each of the four 19-mer templates (160 pmole) with addition of 10×STE (100 mM NaCl and 5 mM EDTA for 1×) in a final volume of 50 µl. The template-primer mixture was incubated for 10 min at 95°C, 5 min at 55°C, 5 min at 22°C and on ice until used.

The template/primer pairs (T/Ps) were extended using RT proteins in a standard dNTP assay reaction. Each assay reaction (20 µl) contained 0.2 pmole (10nM, primer concentration), 2 µl appropriate dNTPs (Amersham, NJ) or extracted cellular dNTPs, 25 mM Tris-HCl (pH 8.0), 100 mM KCl, 2 mM DTT, 5 mM MgCl<sub>2</sub>, 5 µM (dT)<sub>20</sub>, 0.1 mg/ml bovine serum albumin (New England BioLabs). Reactions were initiated by addition of excess RT proteins (60 nM)

in relation to [dNTP] (0.2~6.4 nM or 4~128 fmole in 20  $\mu$ l), and incubated at 37°C for 5 min. Reactions were terminated with 10  $\mu$ l of 40 mM EDTA, 99% formamide. Reaction products were immediately denatured by incubating at 95°C for 5 min and 4  $\mu$ l of each 30  $\mu$ l final reaction mixture was quantitated by PhosphorImager analysis (PerkinElmer, MA) of 14% polyacrylamide-urea denaturing gels (SequaGel, National Diagnostics, GA; Model S2 Sequencing Gel Electrophoresis Apparatus, Labrepc, PA). Note that in our purification protocol, approximately 30–60% of the purified RT protein is active as determined by our pre-steady state kinetic assay using a similar 18-mer/40-mer primer/RNA template (17,18). The reaction with less RT (i.e. 10 nM), which is still a higher concentration than the highest dNTP concentration used (6.4 nM), gave a similar incorporation profile under the assay condition.

**Standard curves for single nucleotide incorporation:** The gels obtained from the incorporation assay (Fig. 1a) were subjected to PhosphorImager analysis (see above). The percent of primer extension in each reaction was calculated by determining the ratios of extended versus total (extended + unextended) primers. Each signal for the extended products was normalized using the background signal in the control reactions incubated without RT (lane C in Fig. 1c). The calculated percentage primer extension was plotted from triplicate reactions, as a function of the dNTP quantity used, generating standard curves for all four dNTPs. The percentage primer extension determined in triplicate reactions containing extracted cellular dNTPs was then extrapolated to the standard curves in order to determine the dNTP contents present in the cellular samples.

**Primer extension by RT proteins:** The primer extension assay was modified from a previously described misincorporation assay (18). Briefly, an RNA template-primer (T/P) was prepared by annealing a 38-mer RNA (5'-AAGCUUGGCUGCAGAAUAUUGCUAGCGGGAAUUCGGCGCG-3', Dharmacon Research, CO) to the 17-mer A primer (5'-CGCGCCGAATTCCT-3'; template:primer, 2.5:1, Invitrogen, CA) <sup>32</sup>P-labeled at the 5' end by T4 polynucleotide kinase (New England BioLabs, MA). Assay mixtures (20  $\mu$ l) contained 10 nM T/P, the RT protein concentrations specified in the individual figure legends, 4 dNTPs at concentrations indicated in the figure legends under the condition described in the dNTP assay above. Reactions were incubated at 37°C for 5 min and terminated for analysis as described in the dNTP assay. Concentrations of RTs (i.e. 1X and 4X) and dNTPs (i.e. 4  $\mu$ M and 0.04  $\mu$ M) used in each primer extension experiment were described in each figure legend. This reaction condition allows multiple rounds of primer extension. We also performed the single round primer extension. In this reaction, RTs were preincubated with the <sup>32</sup>P-labeled 17-mer/38-mer RNA template (10nM), and the reaction was initiated by adding a mixture of dNTP (0.04  $\mu$ M) and a molar excess of cold T/P (1  $\mu$ M) for 3 min at 37°C. For the trap control, RTs were preincubated with a mixture of the <sup>32</sup>P-labeled T/P and the cold T/P, and the reaction was initiated by adding dNTP (0.04  $\mu$ M). We also employed a 120nt long RNA template annealed to a <sup>32</sup>P-labeled 20-mer primer (19). This T/P was also extended by different concentrations of RTs and dNTP for 10 min at 37°C (see figure legend for Fig. 1D).

**Steady state kinetic analysis of dNTP incorporation:** The steady-state kinetic assay protocol described by Boosalis et al. (20) was modified to determine DNA polymerization efficiencies of DNA polymerases with the 18-mer/19-mer template/primers used in the dNTP assay (see above). Reaction conditions were the same as those described in the dNTP assay except for DNA polymerase (0.5~2 nM) concentrations. For the analysis of dNTP incorporation kinetics, four different templates (5' template nucleotide T, C, G, or A for dATP, dGTP, dCTP and dTTP incorporation, respectively) annealed to the <sup>32</sup>P-labeled 18-mer primer were used (see above). The amounts of RTs and incubation time were adjusted to yield extension of 30~60% of the total labeled primer (0.8 pmole) at the highest dNTP concentrations, and the reactions were repeated with 8 decreasing concentrations of each dNTP (for HIV-1 RT, 5, 10, 20, 40, 80, 160,

320 and 720 nM dNTPs and for MuLV RT, 1, 2, 4, 8, 16, 32, 64, and 128  $\mu$ M). We also measured the steady state kinetic values using the processive reverse transcription with the 38-mer RNA annealed to the  $^{32}$ P-labeled 17mer. In this analysis, the different concentrations of the all four dNTP mixtures were used. Products (single nucleotide incorporated primer or all extended products) were resolved in 14% polyacrylamide-urea gel and quantitated by PhosphorImager analysis using the OptiQuant software (PerkinElmer). The  $k_{cat}$  and  $K_M$  values were determined from the Michaelis-Menten equation.

**dNTP extraction from cells:** The protocol for dNTP extraction from cells was similar to that previously described (21). Briefly, cell pellets ( $5 \times 10^4$ – $2 \times 10^6$  cells) were washed twice with 1 X DPBS (Mediatech, VA), and resuspended in 100  $\mu$ l of ice-cold 60% methanol. Samples were vortexed vigorously to lyse the cells and then heated at 95°C for 3 minutes, prior to centrifugation at 12,000 $\times$ g for 30 s. The supernatants were collected and completely dried under vacuum, using a SpeedVac (Savant, NY) with medium heat. The dried pellets were subsequently resuspended in dNTP buffer (50 mM Tris-HCl, pH 8.0 and 10 mM MgCl<sub>2</sub>; 100  $\mu$ l for  $1 \times 10^6$  HeLa cells, and 10  $\mu$ l for  $1 \times 10^6$  primary cells) and usually 1–2  $\mu$ l of the extracted dNTP samples were used for each 20  $\mu$ l single nucleotide incorporation reaction (see above). The proper dilutions of the dNTP samples were prepared for the assay in order to make the primer extension values lie within the linear ranges of the dNTP incorporation (2–32% primer extension). The extracted dNTP samples were stored at –70 until used. Several different volumes of the extracted dNTP samples were also used to confirm the linearity of the primer extension. In addition, the dNTP samples were prepared from different cell numbers, depending on the recovery efficiency of the primary cells from each blood sample (see below). However, the dNTP content of each cell type was normalized by pmole/ $1 \times 10^6$  (see Fig. 1F).

**Isolation and culture of human T cells and monocyte-derived macrophages:** Human macrophages and CD4<sup>+</sup> T cells were isolated from human buffy coats (Blood Research Institute, MA) as described (22). Peripheral blood mononuclear cells were harvested from Ficoll density gradients (Lymphoprep, Axis-Shield PoC AS, Oslo, Norway), and monocytes were then purified using immunomagnetic selection with anti-CD14 antibody conjugated magnetic beads, following the manufacturer's recommendations (Miltenyi Biotech, CA). CD4<sup>+</sup> lymphocytes were isolated from monocyte-depleted buffy coats by immunomagnetic selection using anti-CD4 antibody conjugated magnetic beads (Miltenyi Biotech). The purified human monocytes were incubated in 10 cm dishes in RPMI 1640 (Mediatech, VA) containing 20% Human AB Serum (Sigma, MO) for 4 days in the presence of 5 ng/ml human recombinant GM-CSF (R & D Systems, MN) and then incubated for an additional 3 days in the absence of GM-CSF, to allow differentiation into macrophages. The purified resting T cells were maintained in RPMI 1640 medium supplemented with 10% autologous human serum, while activated T cells were propagated in RPMI 1640 medium supplemented with 10% autologous human serum and 5 ng/ml PHA (Sigma) for 24h, and then incubated in RPMI-1640 medium with 10% human serum and 5ng/ml human, recombinant IL-2 (Sigma) for 3 days. These cell preparations were to prepare dNTP extracts and for the analysis of cell volumes using confocal microscopy.

**Pseudotyped Virus Cloning and Preparation:** pHCMV-VSVG envelope vector (23) and pD3-GFP transfer vector, which encodes the HIV-1 NL4-3 genome with the eGFP gene in place of HIV-1 env, were used for preparing pseudotyped HIV-1. The V148I and Q151N mutations were cloned into pD3-GFP (pNL4-3 based) vector using the overlapping PCR with proper primers designed based on the pNL4-3 RT sequence. The created mutations were confirmed by sequencing with the 3305 Primer (5'–GCACTATAGGCTGTACTGTCC–3'), and correct *Swa*I religation was confirmed with D3-GFP SEQ *Swa*I F (5'–CAGGCCATATCACCTAG–3') and D3-GFP SEQ *Swa*I R (5'–TCTAAC TGGTACCATAAC–3') primers. 293FT cells (Invitrogen, CA) were grown to about 90%

confluency with DMEM, 10% FBS, and 500 µg/ml geneticin in T-175 flasks and transfected with 5 µg envelope vector and 25 µg transfer vector using Lipofectamine 2000 (Invitrogen) as per the manufacturer's recommendations (in the absence of geneticin). Cells were split in half into two new T-175 flasks 16 hours post-transfection. Supernatant was collected 48 and 72 hours post-infection and stored at 4°C. Virus was harvested by ultracentrifugation for 2 hours at 4°C and 22,000 rpm with the Beckman SW28 Rotor. Virus was titered by infection of HeLa cells [obtained through the AIDS Research and Reference Reagent Program, Division of AIDS, NIAID, NIH from Dr. Richard Axel (24)] in the presence of polybrene and infection monitored by fixation and flow cytometry analysis for GFP expression 48 hours post-infection. p24 levels were also measured using the HIV-1 p24 Antigen ELISA Test System (Beckman Coulter, CA).

As a control, transfections were also performed in the absence of the pHCMV-VSV-G vector and this virus was titered on HeLa cells revealing no detectable GFP expression. In addition, controls were performed by pre-treating HeLa cells for 2-hours prior to and during infection with 0.5mM cyclohexamide (CHX), which is a general translation inhibitor. Cells were fixed and analyzed by flow 48 hours post-transfection. Results showed that very little protein was carried over with the pseudotyped virus preparations as evidenced by less than 1% GFP positive cells with plus CHX infections compared to >20% GFP positive cells in minus CHX infections (data not shown).

**Infection of Primary CD4+ T cells and monocyte-derived macrophage:** T cells and macrophage were purified essentially as described above.

T cell infections: After 5 days of T cell stimulation with PHA and IL-2 (see above)  $2 \times 10^5$  stimulated T cells were infected in the presence of polybrene with an MOI of 100 based on HeLa cell titering. For QN virus infections an MOI of 65 was used due to trouble generating high titer QN virus. These infections reflect addition of viral stocks containing 200–300 ng of p24. Infected cells were incubated at 37°C and 5% CO<sub>2</sub> in a 100 µl total volume. Two hours post-infection 100 µl RPMI with 10% heat-inactivated human AB Serum and 4ng/µl IL-2 was added and infections were incubated for an additional 46 hours. Cells were visualized and photographed by fluorescent microscopy in order to detect GFP fluorescence by infected cells. Percent infection was determined after cells were prepared for flow analysis by fixation with 0.5% formaldehyde.

Macrophage infections: After initial magnetic bead purification,  $2 \times 10^6$  CD14+ cells were plated per well into 6-well plates and cultured in RPMI with 2% heat-inactivated Human AB Serum and 5ng/ml GMCSF for 48 hours followed by 48-hour incubation in RPMI with 20% heat-inactivated Human AB Serum and 5ng/ml GMCSF. Cells were then incubated for an additional 8 days in the absence of GMCSF with fresh media added after the initial 4 days. Macrophages were infected with pseudotyped virus at an MOI of 40 based on HeLa cell titering and assuming  $1 \times 10^6$  cells per well in the presence of polybrene. These infections reflect the addition of viral stocks containing 80–130 ng of p24. Initial infections were in 250 µl volume for the first 2 hours at 37°C and 5% CO<sub>2</sub> followed by addition of 2ml RPMI with 20% heat-inactivated human AB serum. Incubations were continued for up to 6 days and cells were periodically examined for GFP fluorescence by fluorescent microscopy. Cells were fixed in 0.5% formaldehyde after disassociation from the plates by 30 min incubation with 2mM EDTA and gentle scraping. Percent infection was determined by flow cytometry.

## Results and Discussion

### Determination of dNTP levels in HIV-1 target cells: human macrophages, and resting or activated CD4+ T cells.

First, we established a highly sensitive enzymatic dNTP assay that allowed us to measure the dNTP contents of primary and non-dividing cells such as macrophages. For the enzymatic measurement of each dNTP contained in a mixture of four different dNTPs, we designed a <sup>32</sup>P-labeled 18-mer primer that can anneal to any of four different 19-mer DNA templates (see Methods). Since these dNTP assay template:primers (T/Ps) contain only one of the four possible nucleotides at the 5' protruding end of the template, DNA polymerases can incorporate only the complementary dNTP onto each of the four T/Ps. Using the specific T/Ps, we found that HIV-1 RT efficiently performed single nucleotide incorporation, even at very low dNTP concentrations, compared to Klenow fragment (KF) of *E. coli* DNA polymerase I (Data not shown) and MuLV RT (see below). When 200 fmole of T/Ps were extended by HIV-1 RT (60 nM) in the presence of different amounts of the individual dNTPs for 5 min at 37°C, 19-mer extended products were generated. As shown in Fig. 1A, incorporation of dCTP and dTTP were detected at concentrations as low as 4 fmole, which extended approximately 2% of the primers. Similar profiles were seen with dGTP and dATP (data not shown). The percent of primer extension in each reaction was then calculated in order to generate standard curves for incorporation of each dNTP onto the appropriate template/primer (see Fig. 1B for TTP and dGTP). No detectable primer extension was observed in control reactions lacking either HIV-1 RT or the required dNTP ("C" in Fig. 1C). The single nucleotide primer extension reaction for each of the four dNTPs was found to be linear for dNTP quantities between 4 and 128 fmole (0.2–6.4 nM), as shown in the standard curve with dTTP and dGTP (Fig. 1B), as well as with dATP and dCTP (data not shown). The linear dNTP incorporation appeared to be affected at higher dNTP amounts in some cases (see 128 fmole TTP in Fig. 1B) because the observed primer extension levels with 128 fmole dNTPs (55~60%) were lower than expected (64% at 128 fmole). Therefore, the upper dNTP limit of the assay should be 128 fmole. This suggested that the dNTP content measurement with the dNTP samples extracted from cells should be performed within the linear dNTP ranges (4~64 fmole dNTP or 2~32% of primer extension). The minimum detection of the dNTP content in this HIV-1 RT based assay (4 fmole) is 25 and 500 times more sensitive than the KF (0.1 pmole (21)) and HPLC (>2 pmole (25–28)) based assays that have previously been used for dNTP content measurement, respectively.

These reactions contained excess HIV-1 RT in relation to substrates, allowing depletion of provided dNTPs within the linear range, as shown in Fig. 1. There are two lines of evidence to support this: 1) The assay was performed at 10 and 20 minutes and no additional primer extension compared to the 5 minute standard reaction was observed (data not shown). 2) The assay showed a 1:1 correlation between the amount of extended primer and the amount of dNTPs included in the reaction, particularly at the low dNTP amount [e.g. 4 fmole of dCTP added resulted in 2% primer extension (4 fmole)].

dNTP samples obtained from cells contain all four dNTPs as well as structurally related rNTPs, which may be present in cells at concentrations up to 200–1000 fold higher than the dNTPs (1). Thus, it is conceivable that an enzymatic dNTP assay might be influenced by the presence of such a vast excess of rNTPs. This is unlikely in the case of HIV-1 RT, which has been shown to incorporate rNTPs very inefficiently (i.e., only when their concentration is at least 0.5 mM) (29). Nonetheless, we tested our assay by adding rNTPs at a concentration 10,000 times higher than the highest dNTP concentration in the linear range of the assay and did not detect any rNTP incorporation (Fig. 1C). A second potential concern with using a primer extension reaction based on the HIV-1 RT is that this enzyme is known to be error-prone (i.e., to be capable of incorporating incorrect dNTPs) (30,31). We therefore tested whether incorrect dNTPs could be incorporated under the assay conditions used. For this test, the dGTP-specific

primer/template pair was extended in the presence of a mixture of 0.5  $\mu\text{M}$  of each of the three incorrect dNTPs (i.e., dATP, dCTP and dTTP); this incorrect dNTP concentration is approximately 100-fold higher than the highest correct dNTP concentrations that showed linear incorporation under these assay conditions (6.4 nM dGTP). As shown in Fig. 1C, no incorporation of incorrect dNTPs was observed even at this artificially high concentration of incorrect dNTPs. In fact, HIV-1 RT needs  $\sim 200 \mu\text{M}$  of incorrect dNTPs to carry out misincorporation under similar reaction conditions (32,33). Therefore, “incorrect” dNTPs and rNTPs present in cellular dNTP samples should not interfere with the determination of individual dNTP levels under the assay conditions established.

We used the HIV-1 RT based assay to examine dNTP levels in the major primary target cells for HIV-1 (i.e., human monocyte-derived macrophages, and activated or resting CD4+ T cells). For this analysis, dNTPs were extracted from these primary cells (see Methods) and the extracted dNTP samples with proper dilutions were used as the dNTP source in single nucleotide extension assays with each of the four T/Ps. As shown in Fig. 1D and 1F, human macrophages were found to contain approximately 4- and 20-fold less dNTPs than resting and activated T cells, respectively. The dNTP content of T cells determined in this assay was found to be similar to that previously determined by the KF based assay (21). We also confirmed the dNTP content of human resting CD4+ T cells using the KF-based assay previously established, but this assay required 10~20 times more cells per assay, due to the higher assay sensitivity limit (0.1 pmole).

Next, we tested the non-specific inhibition of the HIV-1 RT activity by other chemicals co-extracted with cellular dNTPs under the dNTP assay condition. For this test, we performed the dNTP assay with either only pure dNTP (64 or 8 fmole dTTP for the macrophage sample and 16 fmole dGTP for the T cell samples: See Fig. 1E) or mixtures of pure dNTP and the extracted dNTP samples used in Fig. 1D. As shown in Fig. 1E, even with 2  $\mu\text{l}$  of the macrophage extract sample, which contains 16.8 fmole dTTP (Fig. 1F), the primer extension with 64 fmole dTTP was not reduced. Rather, a slight increase ( $\sim 7\%$ ) was observed in the reaction with this mixture, compared to the reaction with only pure dTTP (30.1%). This increase likely resulted from the additional incorporation of dTTP contained in the macrophages sample (16.8 fmole), which should give  $\sim 8\%$  primer extension. More obviously, as shown in Fig. 1E, the reaction with the mixture of 8 fmole pure TTP (theoretically giving 4 % primer extension) and 2  $\mu\text{l}$  of the macrophage sample (16.8 fmole TTP giving 8.4% primer extension) showed 12.4% primer extension, whereas the reaction with only pure 8 fmole dTTP showed the expected 4.3% primer extension. The 8.1 % primer extension increase in the reaction with this mixture should result from the incorporation of the 16.8 fmole dTTP (Fig. 1F) contained in the 2  $\mu\text{l}$  of the macrophage sample. As shown in Fig. 1E, the additive primer extension was also observed in the reactions with the mixtures of pure dGTP (16 fmole, 7.6% primer extension) and the resting T cell samples containing 28 (1X and 1  $\mu\text{l}$ ) or 56 (2X and 2  $\mu\text{l}$ ) fmole dGTP (giving additional 14.2 and 27.4 % primer extensions, respectively: Fig. 1E) as well as activated T cells (data not shown). In addition, the expected primer extension increases were seen when the pure dNTPs (Fig. 1E) were added into the reactions with only extracted samples (Fig. 1F or 1D). For example, the reaction with a mixture of 16 fmole pure dGTP, which gave 7.6% primer extension (Fig. 1E), and the resting T cell sample (1X and 1  $\mu\text{l}$ ) containing 28 fmole (giving theoretically 14 % primer extension in Fig. 1F or actual 13.1% primer extension in Fig. 1D) showed 21.8% primer extension (Fig. 1E). This indicates that the 16 fmole pure dGTP, which produces 8% primer extension, contributed to 7.8 (from theoretical primer extension)  $\sim 8.7$  (from actual calculated primer extension) % primer extension increases. Therefore, this result supports that the incorporation of the pure dGTP was not significantly affected by the addition of the extracted sample (2  $\mu\text{l}$ ). Similar cases can be observed with the 2X T cell samples as well as with the macrophage samples, when the data shown in Fig. 1F (with only extracted dNTP sample) and Fig. 1E (with mixtures of pure and extracted dNTPs) are compared. We also performed the polyrA/oligodT based RT assay measuring the  $^3\text{H}$ -TTP incorporation in the

presence or absence of the 2  $\mu$ l cellular dNTPs samples, and in this experiment we did not also observe any reduction of the  $^3\text{H}$ -TTP incorporation by the cellular dNTP samples (macrophages, T cell and HeLa cells: data not shown). Therefore, the data shown in Fig. 1E, together with the observation from the  $^3\text{H}$ -TTP incorporation RT assay, clearly demonstrates that the inhibitory effect against the HIV-1 RT activity by other chemicals contained in the extracted dNTP samples is absent or at least insignificant. In fact, the protocol employed in this assay has been previously established for similar types of enzymatic dNTP assays (21). We also used several different volumes of the extracted dNTP samples for the dNTP measurements, and with these varied amounts of the samples, we observed the expected linear changes in the percent of primer extension. These data allows us to use 1) the percents of the primer extension with the extracted cellular dNTP samples and 2) the dNTP standard curves shown in Fig. 1B for determining the dNTP content in each extracted sample.

Since there is no compartmentalization of cellular dNTPs between the nucleus and cytoplasm (1), the average cell volumes have been used to calculate the cellular dNTP concentrations. The dNTP concentrations in these three human primary cells were then calculated, by taking into account the volumes of these cell types. The cell volumes of human macrophages, resting and activated CD4+ T cells were calculated using confocal microscopy and found to be 2660, 186 and 320  $\mu\text{m}^3$ , respectively, which are similar to previously published estimates (34–36). Therefore, the calculated dNTP concentrations within human macrophages are approximately 130–250 fold lower ( $\sim 0.026 \mu\text{M}$ ) than in resting and activated CD4+ T cells (3.4  $\mu\text{M}$ , and 6.2  $\mu\text{M}$ , respectively, Fig. 1D).

### Reverse transcription activity of retroviral RTs at dNTP concentrations found in T cells and macrophages.

Lentiviruses differ from oncoretroviruses in their ability to infect non-dividing cells, such as macrophages (11,12). HIV-1 infection of terminally-differentiated, tissue-resident cells of monocytic lineage may be especially important during viral transmission and early replication events (37,38). In contrast, like other RNA tumor viruses, MuLV (11) and AMV [Avian Myeloblastosis Virus, (39,40)] infection requires cell proliferation, AMV infection of chicken embryo-derived macrophages has been described, however, only when these cells were actively dividing as confirmed by  $\text{H}^3$ -thymidine incorporation and mitotic index (39,40). Since the calculated dNTP concentration present in primary macrophages is very low ( $\sim 0.03 \mu\text{M}$ ), we performed a series of experiments employing various substrates and reaction conditions to examine whether lentiviral (HIV-1 and SIV) and oncoretroviral (MuLV and AMV) RTs are able to execute processive DNA synthesis under reaction conditions that contained dNTP concentrations present in macrophages (0.04  $\mu\text{M}$ ) or T cells (4  $\mu\text{M}$ ) (see Fig. 2).

Firstly, a 17-mer primer annealed to a 38-mer RNA template was employed for monitoring reverse transcription. The RT enzymes being compared were then added at two different quantities (4X and 1X); as expected, these different levels of input enzyme resulted in approximately 4-fold differences in the amount of fully extended primer ("F" in Fig. 2A, 2B) at the dNTP concentration present in T cells (4  $\mu\text{M}$ ). However, as shown in Fig. 2A and 2B, when the primer extension was performed in presence of 0.04  $\mu\text{M}$  of each dNTP (i.e., the concentration present in macrophages), the two lentiviral RTs still maintained efficient DNA synthesis capabilities (Fig. 2A), whereas the two oncoretroviral RTs showed a dramatic reduction in their ability to conduct multiple rounds of DNA synthesis (Fig. 2B). Note that slightly more reverse transcription activity was added for reactions with MuLV RT in order to demonstrate that, even with more DNA polymerase activity, MuLV RT did not extend the primer efficiently at 0.04  $\mu\text{M}$  dNTP. In addition, reactions were also performed with HIV-1 and MuLV RTs for longer incubation times with 0.04  $\mu\text{M}$  dNTPs and we observed further extension of the primer, implying that all substrate dNTPs were not depleted under these

reaction conditions (data not shown). Therefore, the low levels of primer extension seen for MuLV RT at 0.04  $\mu\text{M}$  dNTP concentrations are not due to depletion of dNTPs.

Secondly, we also examined the dNTP concentration effect on the DNA polymerization of HIV-1 and MuLV RTs under the condition allowing a single round of primer extension. This analysis employed the same reaction condition as described in Figures 2A and 2B (multiple round primer extension) except using a trap that is a 100 fold molar excess of cold T/P. In this reaction, HIV-1 and MuLV RTs (4X concentration) were preincubated with the  $^{32}\text{P}$ -labeled 17-mer primer annealed to the 38-mer RNA template, and then the RT reaction was initiated by adding a mixture of 0.04  $\mu\text{M}$  dNTP and the cold T/P trap. As shown in Fig. 2C, under this single round extension condition with 0.04  $\mu\text{M}$  dNTP, less primer extension was observed in the reaction with HIV-1 RT, compared to the multiple round primer extension by HIV-1 RT at 0.04  $\mu\text{M}$  (Fig. 2A). We also confirmed the single round primer extension by initiating the reaction containing RTs preincubated with both the cold trap and the  $^{32}\text{P}$ -labeled T/P by adding 0.04  $\mu\text{M}$  dNTPs. In this trap control, no primer extension was observed (data not shown), indicating that the data shown in Fig. 2C was generated under the single round primer extension condition. Indeed, as shown in Fig. 2C, HIV-1 RT was still able to perform the single round of the primer extension very efficiently at 0.04  $\mu\text{M}$  dNTP, compared to MuLV RT incorporating not more than one nucleotide. This confirms the dNTP utilization discrepancy between HIV-1 RT and MuLV RT at low dNTP concentrations.

Thirdly, we also used the multiple round primer extension assay using a 120 nt long HIV-1 RNA template annealed to a  $^{32}\text{P}$ -labeled 20-mer primer (19). As shown in Fig. 2D, even with a 4 fold more RT activity (8X), the two oncoretroviral RTs (M, MuLV RT and A, AMV RT) showed significant low primer extension at 0.04  $\mu\text{M}$  dNTP, compared with the two lentiviral RTs (H, HIV-1 RT; S, SIV RT). This result is similar with the ones described in Fig. 1B and 1C using the 38-mer RNA template.

Lastly, we examined the effect of the dNTP concentration on the DNA synthesis kinetics of HIV-1 RT and MuLV RTs comparing the steady-state kinetic parameters of these two RTs measured by a single nucleotide incorporation assay. This experiment was performed on the 18-mer/19-mer primer/template used for the dNTP assay, but with more limiting RT concentrations than those used in Fig. 1A. Fig. 2E demonstrates the qualitative difference between HIV-1 and MuLV RT in the single nucleotide incorporation with varying dNTP concentrations. Initially, RT activity showing ~60% extension at 50  $\mu\text{M}$  dTTP under the standard reaction condition described in Figure 2A was determined, and then the same reactions were repeated at three different lower dTTP concentrations (5, 0.5 and 0.05  $\mu\text{M}$ ). Indeed, as shown in Fig. 2E, at lower dNTP concentrations, HIV-1 RT was able to polymerize single nucleotide incorporation much more efficiently than MuLV RT. Next, the steady-state kinetic parameters  $K_M$  and  $k_{cat}$  were calculated under similar reaction conditions with lower RT activity than used in Fig. 2E. As seen in Fig. 2F, the  $k_{cat}$  values for the two enzymes with the four dNTPs do not vary greatly, while there is a large increase in the  $K_M$  values for the MuLV RT as compared with HIV-1 RT. Furthermore, in processive DNA synthesis assays similar with Fig. 2A and 2B, we also found that the  $K_M$  values of MuLV and AMV RTs were 23- and 20-fold higher than that of HIV-1 RT, respectively, with similar  $k_{cat}$  values between these RTs (Data not shown). Therefore, these data ( $K_M$  differences) confirm that at lower dNTP concentrations HIV-1 RT is able to polymerize DNA more efficiently than MuLV RT.

The data obtained from the various assays shown in Fig. 2 clearly suggest that the lentiviral RTs have evolved to efficiently catalyze DNA polymerization even at very low dNTP concentrations (such as those found in primary macrophages). In contrast, the oncoretroviral RTs may have adapted to efficiently catalyze DNA synthesis only at the much higher dNTP concentrations that are present in actively dividing cells (i.e. 4  $\mu\text{M}$ ).

### HIV-1 replication in human primary target cells with different dNTP concentrations.

In order to examine further the relationship between cellular dNTP content and retroviral replication, we took advantage of two mutated derivatives of the HIV-1 RT, V148I and Q151N, that had recently been shown by pre-steady state kinetic analysis to have severely reduced dNTP binding affinity ( $k_d$ , 25.6 and 234.2 fold respectively), compared to wild type HIV-1 RT, even though these mutants possess wild type levels of catalysis ( $k_{pol}$ ) (14,17). As seen in Fig. 3, we examined the dNTP concentration dependence of processive DNA polymerization by these mutant RTs, as compared to wild-type RT. Each of the RTs exhibited similar levels of activity in reactions that contained high dNTP concentrations (i.e. 5  $\mu$ M in Fig. 3), which is supported by their identical  $k_{pol}$  values. The wild-type HIV-1 RT was also able to efficiently polymerize DNA even at the low dNTP concentrations found in macrophages (Fig. 3A). However, similar to the two oncoretroviral RTs tested above (Fig. 2B), the two mutant HIV-1 RTs were significantly diminished in their ability to conduct processive DNA synthesis at the low dNTP concentrations found in macrophages. The dNTP binding to the active site of the mutant RTs likely becomes a rate limiting step during the steady state primer extension reaction at low dNTP concentrations. Overall DNA polymerization capability at the dNTP concentrations found in macrophages is greatest for wild type RT, followed by V148I RT, and then Q151N RT which displayed the most significant decrease in dNTP-binding affinity (14, 17). Our kinetic analysis demonstrated that, like these HIV-1 dNTP binding mutants, MuLV RT also has a 40~75 fold higher  $k_d$  than wild type HIV-1 RT (data not shown). Basically, these HIV-1 RT dNTP binding mutants kinetically mimic MuLV RT (Fig. 2B).

Next, in order to examine the effect of RT dNTP binding affinity on lentiviral replication in primary cells, we generated pseudotyped HIV-1 vectors that contained an eGFP reporter cassette, and that were isogenic except for the previously defined RT mutations (i.e., Wild type, V148I, and Q151N). The pseudotyped particles were titered on HeLa cells and then equivalent multiplicities of infection (MOIs) were used to infect primary human T cells and macrophages. As seen in Fig. 4A and 4D, all three vectors had similar abilities to transduce activated human T cells and transformed cell lines (i.e. HeLa cells) containing high cellular dNTP concentrations, which is consistent with the efficient polymerization capability of wild type and these mutant HIV-1 RTs at high concentrations (Fig. 2C) and their similar  $k_{cat}$  values (Fig. 2D). In contrast, the vectors containing the V148I (VI) and Q151N (QN) RT mutants were greatly diminished in their ability to transduce primary macrophages even with higher MOI infections (Fig. 4B, C and D). Therefore, this reflects the enzymatic inability of these mutant RTs to synthesize DNA at low dNTP concentrations, and suggests that dNTP binding affinity of lentiviral RTs is a key contributor to viral replication in macrophages.

In summary, using both biochemical and virological analyses, we were able to investigate the relationship between cellular dNTP pools, RT binding affinity for dNTPs, and viral replication in non-dividing host primary cells that contain limiting dNTP concentrations. Our results strongly suggest that the enzymatic adaptation of the HIV-1 RT DNA polymerase active site to catalyze DNA synthesis in cellular environments that contain low levels of dNTPs is a major contributor to the unique ability of these viruses to efficiently replicate in macrophages. Therefore, this study provides evidence that RT plays an essential role in establishing and maintaining the macrophage tropism of HIV-1 during the course of viral infection, which presents unique virological and pathological characteristics that differentiate lentiviruses from oncoretroviruses.

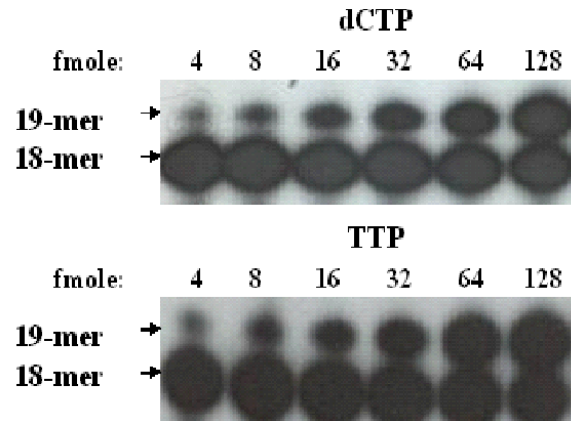
### References

1. Traut TW. Mol Cell Biochem 1994;140:1–22. [PubMed: 7877593]
2. Angus SP, Wheeler LJ, Ranmal SA, Zhang X, Markey MP, Mathews CK, Knudsen ES. J Biol Chem 2002;277:44376–44384. [PubMed: 12221087]

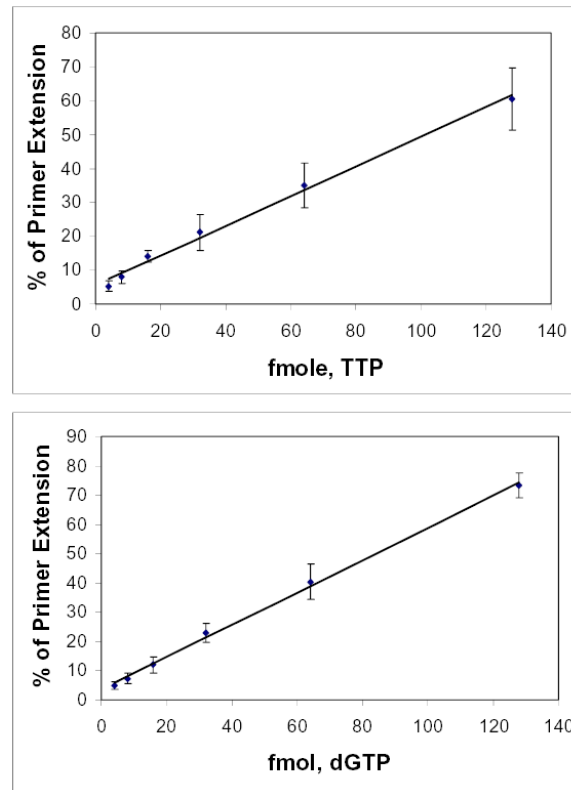
3. Jackson RC, Lui MS, Boritzki TJ, Morris HP, Weber G. *Cancer Res* 1980;40:1286–291. [PubMed: 7053201]
4. Hauschka PV. *Methods Cell Biol* 1973;7:361–462. [PubMed: 4592524]
5. Fuller SA, Hutton JJ, Meier J, Coleman MS. *Biochem J* 1982;206:131–138. [PubMed: 6289810]
6. Skoog L, Bjursell G. *J Biol Chem* 1974;249:6434–6438. [PubMed: 4472692]
7. Zhao X, Chabes A, Domkin V, Thelander L, Rothstein R. *EMBO J* 2001;20:3544–3553. [PubMed: 11432841]
8. Chabes A, Georgieva B, Domkin V, Zhao X, Rothstein R, Thelander L. *Cell* 2003;112:391–401. [PubMed: 12581528]
9. Yao R, Zhang Z, An X, Bucci B, Perlstein DL, Stubbe J, Huang M. *Proc Natl Acad Sci U S A* 2003;100:6628–6633. [PubMed: 12732713]
10. Zhao X, Rothstein R. *Proc Natl Acad Sci U S A* 2002;99:3746–3751. [PubMed: 11904430]
11. Lewis PF, Emerman M. *J Virol* 1994;68:510–516. [PubMed: 8254763]
12. Lewis P, Hensel M, Emerman M. *EMBO J* 1992;11:3053–3058. [PubMed: 1322294]
13. Kim B. *Methods* 1997;12:318–324. [PubMed: 9245612]
14. Weiss KK, Chen R, Skasko M, Reynolds HM, Lee K, Bambara RA, Mansky LM, Kim B. *Biochemistry* 2004;43:4490–4500. [PubMed: 15078095]
15. Diamond TL, Kimata J, Kim B. *J Biol Chem* 2001;276:23624–23631. [PubMed: 11325971]
16. Malboeuf CM, Isaacs SJ, Tran NH, Kim B. *Biotechniques* 2001;30:1074–1078, 1080, 1082, passim. [PubMed: 11355343]
17. Weiss KK, Bambara RA, Kim B. *J Biol Chem* 2002;277:22662–22669. [PubMed: 11927582]
18. Diamond TL, Souroullas G, Weiss KK, Lee KY, Bambara RA, Dewhurst S, Kim B. *J Biol Chem* 2003;278:29913–29924. [PubMed: 12740369]
19. Balakrishnan M, Roques BP, Fay PJ, Bambara RA. *J Virol* 2003;77:4710–4721. [PubMed: 12663778]
20. Boosalis MS, Petruska J, Goodman MF. *J Biol Chem* 1987;262:14689–14696. [PubMed: 3667598]
21. Roy B, Beuneu C, Roux P, Buc H, Lemaire G, Lepoivre M. *Anal Biochem* 1999;269:403–409. [PubMed: 10222017]
22. Klimatcheva E, Planelles V, Day SL, Fulreader F, Renda MJ, Rosenblatt J. *Mol Ther* 2001;3:928–939. [PubMed: 11407907]
23. Akkina RK, Walton RM, Chen ML, Li QX, Planelles V, Chen IS. *J Virol* 1996;70:2581–2585. [PubMed: 8642689]
24. Maddon PJ, Dalglish AG, McDougal JS, Clapham PR, Weiss RA, Axel R. *Cell* 1986;47:333–348. [PubMed: 3094962]
25. Maybaum J, Klein FK, Sadee W. *J Chromatogr* 1980;188:149–158. [PubMed: 7380929]
26. Huang D, Zhang Y, Chen X. *J Chromatogr B Analyt Technol Biomed Life Sci* 2003;784:101–109.
27. Decosterd LA, Cottin E, Chen X, Lejeune F, Mirimanoff RO, Biollaz J, Coucke PA. *Anal Biochem* 1999;270:59–68. [PubMed: 10328765]
28. Di Pierro D, Tavazzi B, Perno CF, Bartolini M, Balestra E, Calio R, Giardina B, Lazzarino G. *Anal Biochem* 1995;231:407–412. [PubMed: 8594993]
29. Kaushik N, Talele TT, Pandey PK, Harris D, Yadav PN, Pandey VN. *Biochemistry* 2000;39:2912–2920. [PubMed: 10715111]
30. Preston BD, Poesz BJ, Loeb LA. *Science* 1988;242:1168–1171. [PubMed: 2460924]
31. Roberts JD, Preston BD, Johnston LA, Soni A, Loeb LA, Kunkel TA. *Mol Cell Biol* 1989;9:469–476. [PubMed: 2469002]
32. Menendez-Arias L. *Biochemistry* 1998;37:16636–16644. [PubMed: 9843431]
33. Gutierrez-Rivas M, Ibanez A, Martinez MA, Domingo E, Menendez-Arias L. *J Mol Biol* 1999;290:615–625. [PubMed: 10395818]
34. DeFife KM, Jenney CR, Colton E, Anderson JM. *J Histochem Cytochem* 1999;47:65–74. [PubMed: 9857213]
35. Krombach F, Munzing S, Allmeling AM, Gerlach JT, Behr J, Dorger M. *Environ Health Perspect* 1997;105(Suppl 5):1261–1263. [PubMed: 9400735]

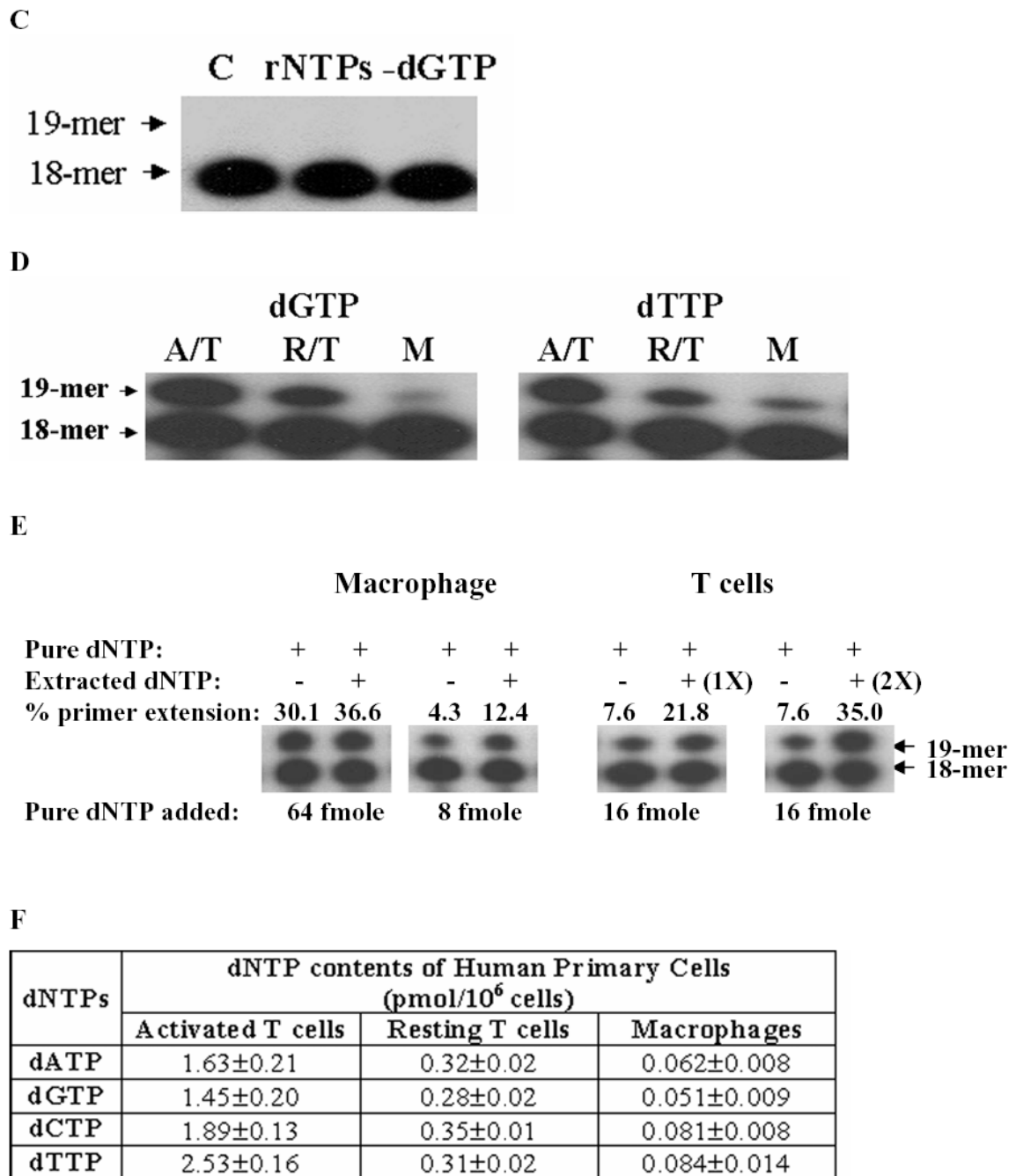
36. Munch-Petersen B, Tyrsted G, Dupont B. *Exp Cell Res* 1973;79:249–256. [PubMed: 4361080]
37. Kinter A, Arthos J, Cicala C, Fauci AS. *Immunol Rev* 2000;177:88–98. [PubMed: 11138789]
38. Moore JP, Trkola A, Dragic T. *Curr Opin Immunol* 1997;9:551–562. [PubMed: 9287172]
39. Durban EM, Boettiger D. *Proc Natl Acad Sci U S A* 1981;78:3600–3604. [PubMed: 6267600]
40. Durban EM, Boettiger D. *J Virol* 1981;37:488–492. [PubMed: 6260997]

A



B



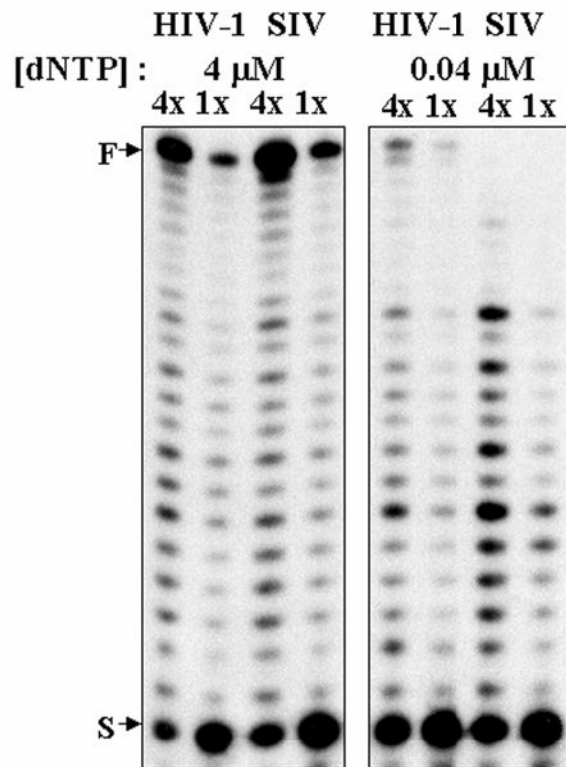


**Figure 1. Primary cell dNTP content determination by the HIV-1 RT-based dNTP assay.**

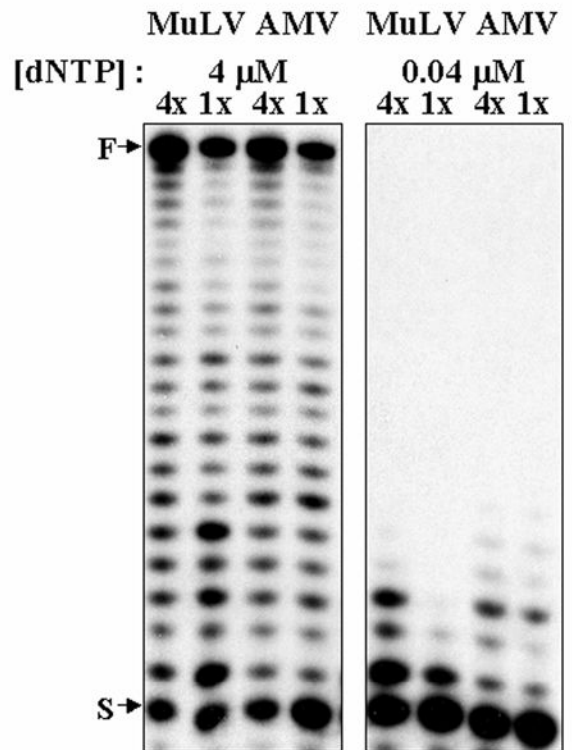
**(A)** dCTP and dTTP incorporation by HIV-1 RT (60 nM) was measured using the dCTP-specific template/primer pair (200 fmole) in the presence of different amounts of dCTP. **(B)** Standard curve for the incorporation of dTTP and dGTP onto the dTTP and dGTP-specific template/primer pairs. The percent primer extension in each reaction was plotted after background normalization (see Methods). Each data point was calculated from three independent reactions; error bars denote the standard deviation from the mean. **(C)** Incorporation of incorrect dNTPs and rNTPs. The G-specific template/primer pair was incubated with HIV-1 RT (60 nM) and 50  $\mu$ M rNTPs (“rNTPs”) or a mixture of three incorrect dNTPs (“-dGTP”; this corresponds to a mixture that contained 0.5  $\mu$ M of each dTTP, dCTP and dATP). **(D)** dNTP samples were

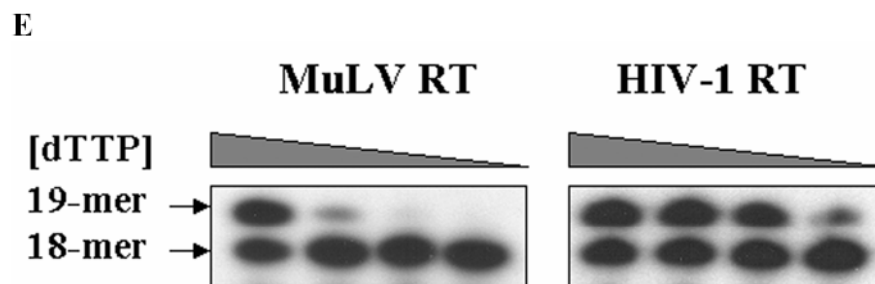
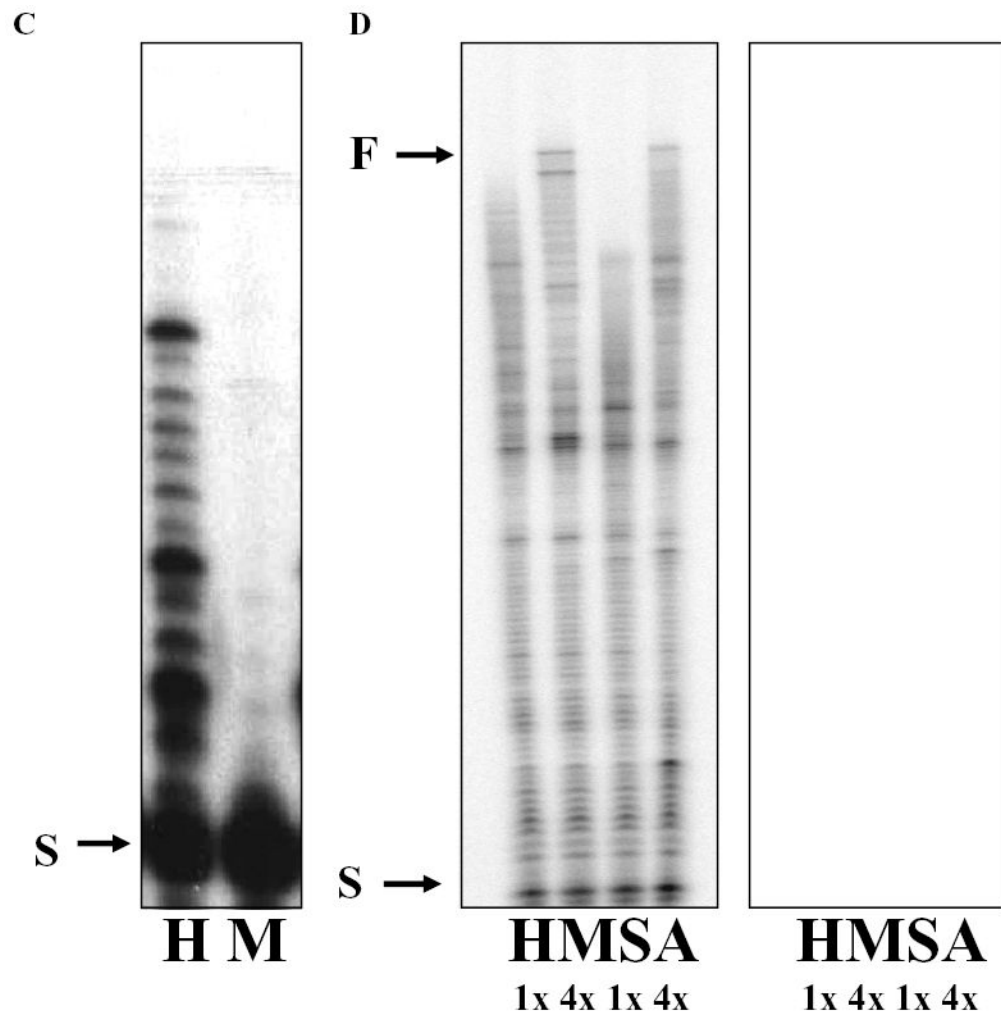
isolated from human activated (A/T) or resting (R/T) CD4+ T cells or CD14+ macrophages (M). dNTP samples contained in 1 (T cells) ~ 2 (macrophages)  $\times 10^5$  cells were used for each assay reaction using dGTP- or dTTP- specific template/primer pairs. (E) Effect of other chemicals contained in the extracted dNTP samples. The dNTP assay was performed with either only pure dNTP or mixtures of pure and extracted dNTPs. The amounts of the pure dNTPs used in the reactions were shown at the bottom of the figure, and 1 (T cells) or 2 (macrophages)  $\mu\text{l}$  of the cellular dNTP sample was used. The percent of primer extension in each reaction is also shown. Two different amounts of the T cell dNTP sample, 1X and 2X, were used. The results for all template/primer pairs with the extracted dNTP samples are summarized in (F). dNTP values shown represent mean values calculated from three independent experiments performed in triplicate; standard deviations are shown for each value. All reactions were performed as described in Methods, and products were analyzed by electrophoresis through 14% denaturing polyacrylamide gels, followed by PhosphorImager analysis (see Methods).

A

**Lentiviral RTs**

B

**Oncoretroviral RTs**



**F**

dNTPs	MuLV RT		HIV-1 RT	
	$K_M$ ( $\mu\text{M}$ )	$k_{\text{cat}}$ ( $\text{min}^{-1}$ )	$K_M$ ( $\mu\text{M}$ )	$k_{\text{cat}}$ ( $\text{min}^{-1}$ )
dGTP	4.96 $\pm$ 0.38	0.32 $\pm$ 0.09	0.0328 $\pm$ 0.007	0.60 $\pm$ 0.03
dATP	29.2 $\pm$ 6.3	0.38 $\pm$ 0.09	0.0641 $\pm$ 0.0003	0.45 $\pm$ 0.04
dTTP	27.5 $\pm$ 6.1	0.43 $\pm$ 0.05	0.0655 $\pm$ 0.025	0.43 $\pm$ 0.07
dCTP	6.52 $\pm$ 1.54	0.42 $\pm$ 0.06	0.1280 $\pm$ 0.023	0.35 $\pm$ 0.05

**Figure 2. Comparison of reverse transcription capability of lentiviral and oncoretroviral RTs at different dNTP concentrations.**

A  $^{32}\text{P}$ -labeled 17-mer primer (S) was annealed to a 38-mer RNA template and then extended by two lentiviral RTs (A), HIV-1 and SIV RTs, and two oncoretroviral RTs (B), MuLV and AMV RTs, in reactions containing 4  $\mu\text{M}$  of each dNTP. Two different input levels of RT activity were used in these reactions (1 $\times$  and 4 $\times$ , as indicated). The RT reactions were repeated with these same two reverse transcription activities (4 $\times$  and 1 $\times$ ) in reactions that contained 0.04  $\mu\text{M}$  of each dNTP; the fully extended primer is 38 nt long (F). 4X concentrations of RTs are as follows: HIV-1 RT, 3.2 nM; SIV RT, 6 nM; MuLV RT, 0.5 nM; AMV RT, 2.25 nM. The same T/P used in (A) and (B) was extended by HIV-1 (3.2nM) and MuLV RTs (0.5nM) under the condition allowing a single round of primer extension at 0.04  $\mu\text{M}$  dNTP (C). A  $^{32}\text{P}$ -labeled 20-mer primer (S) annealed to a 120nt long RNA template encoding HIV-1 RT genome (D) was extended by the four RT under the same condition used in (A) and (B). The 2X concentration was used for the two lentiviral RTs (H, 6.4nM HIV-1 RT and S, 12nM SIV RT), whereas the 8X concentration was used for the two oncoretroviral RTs (M, 4nM MuLV RT and A, 9nM AMV RT). (E) dNTP concentration dependent single nucleotide incorporation by MuLV and HIV-1 RTs was determined on the 18-mer/19-mer assay T/Ps. The single nucleotide incorporation activity of these two DNA polymerases at different dNTP concentrations was analyzed using the T-specific template/primer pair (10 nM) in the presence of decreasing dTTP concentrations (50, 5, 0.5, and 0.05  $\mu\text{M}$ ). The 18-mer and 19-mer primers indicate unextended and extended primers, respectively. Polymerase concentrations showing approximately 60% primer extension on this template/primer pair at 50  $\mu\text{M}$  TTP are MuLV RT, 1 nM and HIV-1 RT, 0.8 nM. (F) Steady state kinetic analysis of the two DNA polymerases with the four 18mer/19mer T/Ps is shown (see Methods). Results are from experiments performed in triplicate with standard deviations.

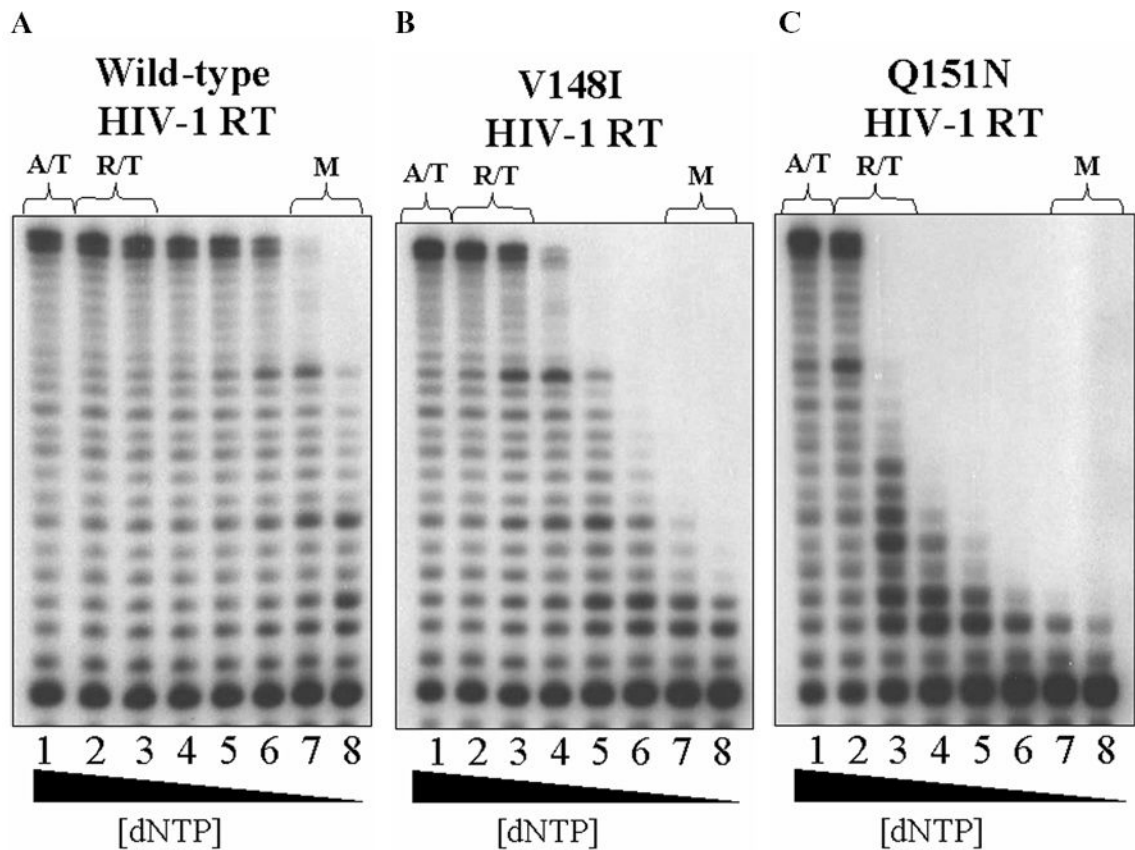


**Figure 3. dNTP dependence of HIV-1 WT (A), V148I (B), and Q151N (C) RT mutants during multiple round polymerization.**

The  $^{32}\text{P}$ -labelled 17-mer primer annealed to the 38-mer RNA template was extended by equivalent activities of the three RTs (as determined by analysis of enzymatic activity under reaction conditions that contained  $5\ \mu\text{M}$  of each dNTP). Reactions were then conducted with decreasing equimolar concentrations of all four dNTPs, and were analyzed on a 14% denaturing polyacrylamide gel. Lanes 1–8 correspond to 5, 2.5, 1, 0.5, 0.25, 0.1, 0.05, and  $0.025\ \mu\text{M}$  concentrations of all four dNTPs, respectively. Reactions performed at concentrations that represent those found in activated (A/T) and resting (R/T) T cells and macrophages (M) are marked.

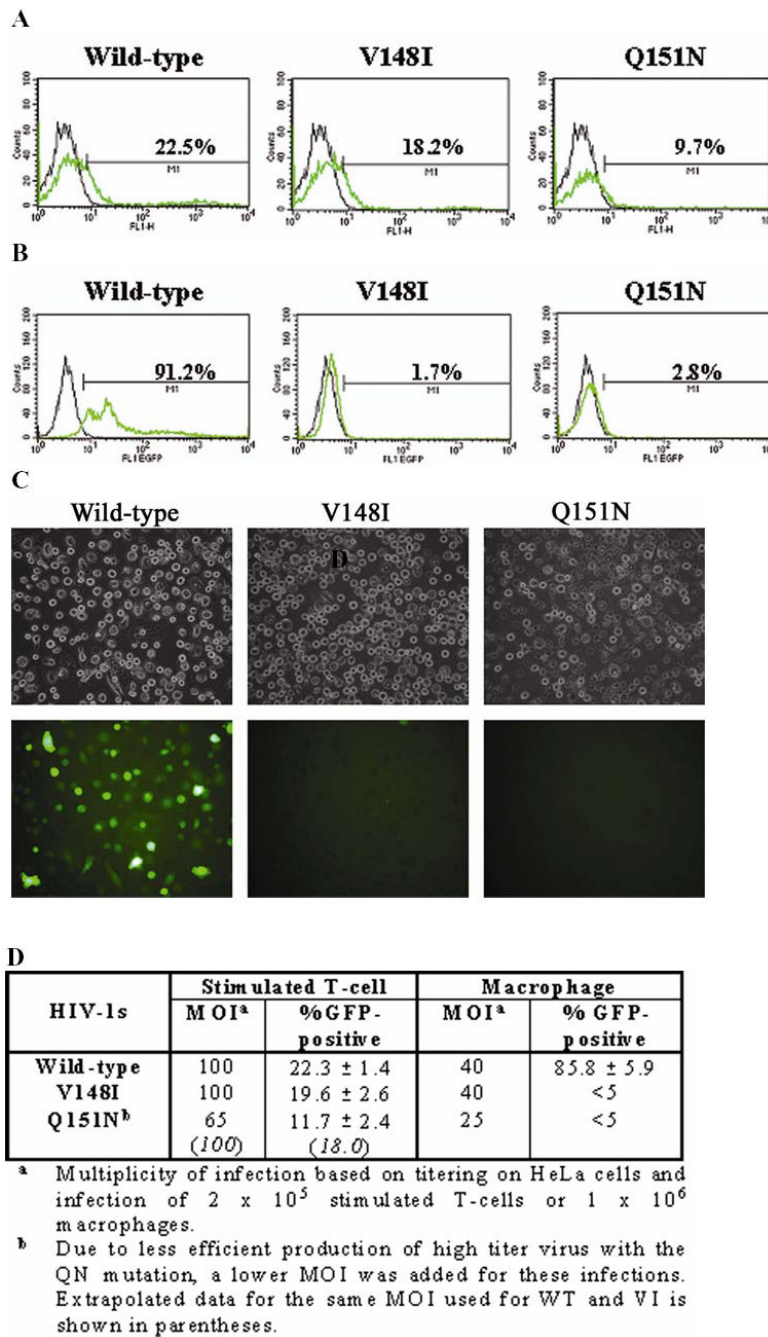


**Figure 4. Transduction of primary human cells by pseudotyped lentivirus vectors containing WT, V148I, or Q151N RTs.**

Primary human cells were infected with eGFP-encoding lentivirus vectors containing the indicated RT variants (WT, V148I, Q151N). T cells were fixed 48h post-infection with 0.5% formaldehyde and macrophages were fixed 120h post-infection in 0.5% formaldehyde after treatment with 2mM EDTA and gentle scraping. Flow cytometric analysis of eGFP expression in transduced CD4<sup>+</sup> T cells (**A**) and macrophages (**B**) from one representative experiment are shown. The negative control (mock) infections are shown in black, while results from vector-transduced cells depicted by the green histograms. Total cells were gated on the basis of physical parameters (forward and side scatter) and the percent GFP-positive cells was

determined after setting gating parameters such that the %-GFP positive in the negative control cells was 1%. **(C)** Representative images of macrophages 120h post-infection are shown. Fluorescent images are shown below (upper panels) with corresponding bright field images (lower panels); images were taken at 14× magnification. A summary of flow cytometric results from one experiment performed in triplicate is also shown in **(D)**.